UDC544.653.2/.3
DOI: 10.15587/1729-4061.2018.127764

DEFINITION OF THE AGING PROCESS PARAMETERS FOR NICKEL HYDROXIDE IN THE ALKALINE MEDIUM

V. Kotok
PhD, Associate Professor**
Department of Processes, Apparatus and General Chemical Technology*
E-mail: valeriykotok@gmail.com
V. Kovalenko
PhD, Associate Professor**
Department of Analytical Chemistry and Food Additives and Cosmetics*
E-mail: vadimchem@gmail.com
*Ukrainian State University of Chemical Technology
Gagarina ave., 8, Dnipro, Ukraine, 49005
**Department of Technologies of Inorganic Substances and Electrochemical Manufacturing
Vyatka State University
Moskovskaya str., 36, Kirov, Russian Federation, 610000

Визначено параметри процесу старіння гідроксиду нікелю в лужному середовищі в залежності від часу зберігання та наявності активуючої добавки гідроксиду кобальту. Показано, що процес старіння зумовлений рекристалізацією гідроксиду нікелю під час зберігання, а також що цей процес йде через впорядкування дефектів кристалічної решітки у тому числі у напрямку площини (001). Визначено, що впродовж зберігання коефіцієнт використання порошку гідроксидунікелю істотно зменшується

Ключові слова: старіння, гідроксид нікелю, $Ni(OH)_2$, $Co(OH)_2$, лужний акумулятор, коефіцієнт використання, дефект, кристалічна решітка

Определены параметры процесса старения гидроксида никеля в щелочной среде в зависимости от времени хранения и наличия активирующей добавки гидроксида кобальта. Показано, что процесс старения обусловлен рекристаллизацией гидроксида никеля при хранении, а также что процесс идет через упорядочение дефектов кристаллической решетки,в том числе в направлении плоскости (001). Определено, что в течение хранения коэффициент использования порошка гидроксида никеля значительно уменьшается

Ключевые слова: старение, гидроксид никеля, $Ni (OH)_2$, $Co(OH)_2$, щелочной аккумулятор, коэффициент использования, дефект, кристаллическая решетка

1. Introduction

In the modern world, the accumulator systems have become an integral part of technology. Accumulators are the only small and autonomous devices that can provide electrical current independently of external conditions. Owing to this, a large number of experimental scientific papers are devoted to the study of aspects and issues related to operation and increase of specific characteristics of accumulators.

Despite the appearance of conceptually new systems that can be used for storage of electrical energy, the work on improving traditional, or so-called “classic” systems is still ongoing.

One of the “classic” accumulator systems are alkaline accumulators with positive nickel oxide electrode [1]. They include Ni–Cd, Ni–MH, Ni–Zn, Ni–Fe systems, and also $Ni–H_2$ [2]. All listed types of chemical power sources find a wide range of applications, owing to high specific characteristics, long cycle life, wide range of operating temperatures. Electronics, driving accumulators, power sources for spacecrafts – is a far from complete list of applications for these systems. The main element used in these accumulators is nickel oxide electrode or nickel electrode. The core of this electrode is nickel hydroxide, the properties of which determine specific characteristics of the whole device. It should also be noted that nickel oxide electrode is also used in supercapacitors [3, 4]. Nickel hydroxide can be deposited onto a transparent electrode as a thin, transparent film with controllable optical properties. [5, 6]. Such electrodes can be used in so-called “smart windows” and “smart mirrors”.

The application of nickel hydroxide is not limited to chemical power sources. Nickel-based layered double hydroxides, precipitated in the presence of water-soluble organic dyes, form pigments that are stable under UV-radiation and can be used in paints and lacquers [7]. Electrodes containing nickel hydroxide, nickel oxide, nickel-based layered double hydroxides (oxides) are used as efficient water decomposition catalysts [8]. Also, nickel oxide is widely used for the preparation of new organic compounds [9] and removal of some organic compounds from wastewater [10]. One of the possible applications of nickel oxide electrode as an electrode for methanol fuel cells [11]. Nickel oxide films found their application in photosensitized solar cells [12], nickel hydroxide films – for corrosion protection of some materials [13].

Based on a wide range of application for nickel hydroxide and oxide compounds, the study of their properties is a relevant problem. Solving this problem would enable to improve specific characteristics of devices that use these compounds.

2. Literature review and problem statement

Operation of alkaline accumulator depends on characteristics of nickel hydroxide, which is the active material of nickel oxide electrode. Changes in electrode properties are directly related to structural changes in nickel hydroxide. For nickel hydroxide there are two known polymorphs: α-$Ni(OH)_2$ and β-$Ni(OH)_2$. Some authors also outline an intermediate form – β_{bc}-$Ni(OH)_2$ [14, 4], bc – stands for badly crystalline. All crystal forms of nickel hydroxide and oxyhydroxide have a hexagonal crystal lattice. The difference of α-$Ni(OH)_2$ from β-$Ni(OH)_2$ is the presence of water molecules and acid anions in the interlayer space, and also the difference between crystal lattice parameters, namely c: a=3.08 Å, c=8 Å and a=3.126 Å, c=4.605 Å respectively [15]. Transition from one form to another results in changes of crystal lattice parameters. The most significant change occurs during transition between charged forms γ-NiOOH and β-NiOOH (a=2.82 Å, c=20.65 Å and a=2.81 Å, c=4.84 Å, respectively). These changes can be summarized in a diagram presented in Fig. 1 [16, 17].

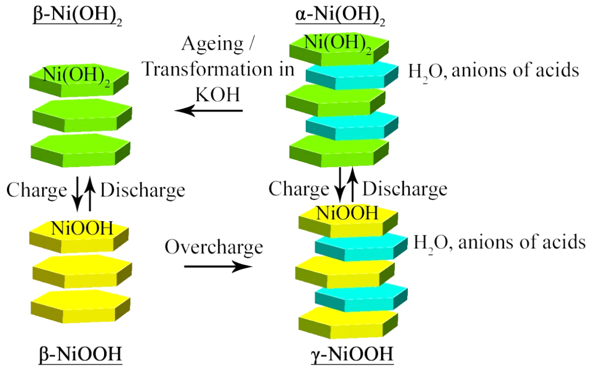

Fig. 1. Changes of active material during operation in the accumulator, according to Bode

Transformation in the base is also called "aging" process [18]. In [19], the aging process is described by consecutive transition $\alpha \rightarrow \beta_{bc}$-$Ni(OH)_2 \rightarrow \beta$-$Ni(OH)_2$. However, the authors of [20, 21], using Raman spectroscopy, have established that all 4 phases depicted in Fig.1 have a common open-packed structure of oxygen atom packing – ABBCCA. Thus, it is stated that during cycling within these 4 structures there are no significant structural changes. In addition, it was also discovered that during "aging", the close-packed ABAB oxygen atom packing is formed. The latter is unstable during regular cycling conditions [16].

Other authors have shown that under regular cycling conditions, the transition occurs between ABAB and ACBA (I) structures, and in case of overcharge and aging — between ACBA and ABBCCA (II) – Fig. 2 [22].

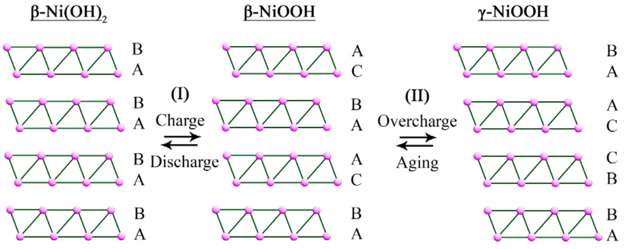

Fig. 2. Structures ABAB, ABCA and ABBCCA. Pink color represents oxygen atoms

In general, two neighboring structures ABAB and ABBCCA differ as shown in Fig. 3. Structures ABAB and ABBCCA are characterized by T1 and P3 oxygen atom packing [23], Fig. 3.

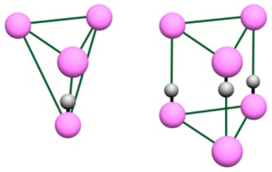

Fig. 3. Structure T1 (ABAB) on the left and P3 (ABBCCA) on the right. Pink color represents oxygen atoms, and grey — hydrogen atoms

Here T1 – oxygen packing, in which hydrogen atom is dislocated from the center, and P3 oxygen packing, in which hydrogen-oxygen bonds lie on the edges of trigonal prisms.

In general, the aging process is not studied in detail and there are several opinions regarding its mechanism. According to the literature [24], the aging is viewed as an Ostwald's ripening process, which consists in dissolution, formation and growth of the crystal. The transformation of α-phase into β-beta phase occurs through a solution. In paper [25], the mechanism of aging in the basic medium is presented as the transition of α-$Ni(OH)_2$/γ-$NiOOH \rightarrow$ β-$Ni(OH)_2$/β-NiOOH through badly crystalline β_{bc}-$Ni(OH)_2$, which then transforms into well-crystalline β-$Ni(OH)_2$. In general, this transition can be represented as α-$Ni(OH)_2 \rightarrow$ β_{bc}-$Ni(OH)_2 \rightarrow \beta$-$Ni(OH)_2$, where phases closer to right show less electrochemical activity.

This causes ambiguity of the presented data. Additionally, no data were found regarding the aging rate or the influence of activating additives to nickel oxide electrode [26, 27]. Thus, determination of aging process parameters could reveal necessary information for the creation of active materials of suppression of the aging process.

According to paper [28], the aging process is determined by the medium in which it occurs, changes the structural-kinetic parameter DS^2 and structure of $Ni(OH)_2$. This parameter affects specific characteristics of the electrode, in which D is the proton diffusion coefficient, and S – specific surface area of nickel hydroxide. However, the influence of process duration and presence of activator – cobalt hydroxide, has not been studied in detail.

3. The aim and objectives of the study

The aim of the study was to determine the parameters of the aging process, including determination of the rate of the aging process and influence of the aging process on characteristics of nickel oxide electrode.

In order to achieve the set aim, the following objectives were formulated:

– to determine the influence of the aging process on changes in the structure of $Ni(OH)_2$, without activation and cobalt-activated, in time, in the solution of KOH;

– to determine the influence of the aging process on electrochemical activity of nickel hydroxide with and without the cobalt surface activator.

4. Materials and method used in the study

Materials used in the study of aging process.

For all experiments, nickel hydroxide synthesized in a slit diaphragm electrolyzer [29] i_c=15.7 A/dm^2 was used. NaOH with a concentration of 24 g/L was used in the anodic chamber, and nickel sulfate solution with a Ni^{2+} concentration of 12.3 g/L was used in the cathodic chamber. The synthesized $Ni(OH)_2$ was immediately filtered from the solution.

As a result, two batches of $Ni(OH)_2$, 30 g each, were prepared, which were subjected to the following treatment.

Treatment of $Ni(OH)_2$ batch without the activator.

1. Drying in an oven at 110 °C, 1 day;
2. Grinding in a mortar;
3. Sifting through a mesh (cell size 71 μm);
4. Aging of nickel hydroxide powder in distilled water for 1 day, followed by filtration and washing (this step was necessary to remove soluble salts);
5. Drying at 110 °C, 1 day.

The powder was then sealed in an air-tight bag. This powder was not subjected to aging and was labeled as NH-0. The rest of hydroxide was split into parts, placed in 50 ml flasks with 4.5 M KOH solution, and aged for a different time.

Treatment of $Ni(OH)_2$ batch with cobalt additive.

For the sample with the activator additive, the stages 1-5 were similar to those described in *“Treatment of $Ni(OH)_2$ batch without the activator”*.

Part of the powder was immediately separated and labeled as NH-BG. This sample was necessary for comparing the influence of treatment differences of $Ni(OH)_2$ and $Ni(OH)_2$ with the addition of $Co(OH)_2$.

Next, the $CoSO_4$ solution with a concentration of 256 g/L, assuming the ratio of Co/Ni 5 % (wt.) was added to the rest of the powder, and the obtained mixture was dried at 110 °C. In order to ensure that treatment of $Ni(OH)_2$ with the activator did not differ from that of the NH-BG sample, distilled water was added instead of $CoSO_4$, and dried at 110 °C.

In order to obtain $Co(OH)_2$ on the surface of nickel hydroxide, the powder with cobalt salt was passed through 4.5M KOH and the thoroughly washed with water. After all operations, the powder was dried at 110 °C.

Part of $Ni(OH)_2$ powder with $Co(OH)_2$ that was not subjected to aging, was packed into the airtight bag and labeled as NHC-0.

The rest of $Ni(OH)_2$ powder with $Co(OH)_2$ was split into parts, which were placed in 50 ml flasks with 4.5M KOH and aged for a different time.

After aging in alkali, the powders were washed with distilled water until pH=7 and dried at 110 °C.

Sample labels and aging conditions are summarized in Table 1.

Structural analysis of the samples.

The structure of all prepared samples was evaluated by means of X-ray diffraction analysis. The XRD patterns were recorded using the DRON-3 diffractometer (Russia) (Co-Kα radiation).

Analysis of electrochemical activity of nickel hydroxide powders.

In order to evaluate the electrochemical activity, the samples were subjected to galvanostatic charge-discharge cycling, from the results of which the active mass utilization coefficient was calculated.

Table 1

Aging conditions and sample labels

Label	NH-0	NH-1	NH-2	NH-3	NH-4	NH-5	–	–
Composition	NH*	NH	NH	NH	NH	NH	–	–
Aging time, days	0	7	14	28	42	56	–	–
Label	NH-BG	NHC-0	NHC-1	NHC-2	NHC-3	NHC-4	NHC-5	NHC-6
Composition	NH	NH, A*	NH, A	NH, A	NH, A	NH, A	NH, A	NH, A
Aging time, days	0	0	7	14	30	35	42	56

*Notes: *– NH – nickel hydroxide, $Ni(OH)_2$; A – activator, $Co(OH)_2$*

Charge-discharge cycling was conducted using the cell shown in Fig. 4.

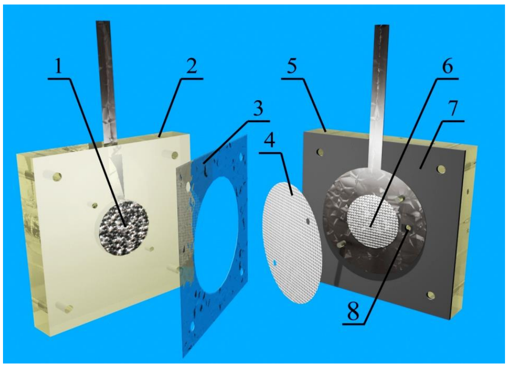

Fig. 4. Design of experimental cell: 1 – nickel foam counter-electrode; 2 – first Plexiglas half-element; 3 – polyethylene gasket; 4 – Nylon 6 separator; 5 – second Plexiglas half-element; 6 – working electrode – nickel foil with nickel mesh welded onto it; 7 – rubber gasket; 8 – hole for the introduction of capillary

The nickel hydroxide samples were mixed with graphite and PTFE to prepare active mass, which was pasted onto the working electrode, in order to conduct electrochemical studies. The active mass composition is listed in Table 2.

Table 2

Composition of active mass

Name	Type	ω (wt.), parts.
Nickel hydroxide	–	0.81
Graphite	GAK-3	0.16
PTFE	F-4D suspension	0.03 (dry matter)
TOTAL	–	1

Cadmium electrode with higher capacity was used as a counter-electrode, Ag/AgCl (KCl sat.) was used as a reference electrode. The cell and the reference electrode were connected via Luggin capillary, filled with 4.5 M KOH.

The theoretic capacity of the working electrode was calculated from the mass of nickel hydroxide on the pasted electrode, with the electrochemical equivalent calculated with the assumption of single electron transfer:

$$Q_t = \frac{\Delta m_e \cdot \omega_{Ni(OH)_2}}{K_{Ni(OH)_2}}, \qquad (1)$$

where Q_t – theoretic capacity of the electrode, A·h; $K_{Ni(OH)_2}$ – electrochemical equivalent, 3.46 A·h/g; $\omega_{Ni(OH)_2}$ – content of the active material, 0.81; Δm_e – weight of active mass on the electrode, g.

Charge current was calculated based on charge time and overcharge coefficient (which accounts for side reaction of O_2 evolution on charge):

$$I_c = \frac{Q_t}{T_c} \cdot k, \tag{2}$$

where I_c – charge current, A; k – overcharge coefficient, 1.5; T_c – charge time, 18 hours.

The discharge current was calculated based on the five-hour regime:

$$I_d = \frac{Q_t}{T_d}, \tag{3}$$

where I_d – discharge current, A; T_d – discharge time, 5 hours.

The discharge characteristics were recorded onto a computer using a high ohm (20 MOhm) multimeter UNI-T UT-70B (China). The discharge characteristic was represented as a dependency of potential on utilization coefficient (K_u). For this, the X-axis was obtained by dividing time by theoretic discharge time, which was 5 hours.

5. Structural analysis of nickel hydroxide powders with and without the activator, which were aged for a different time

The XRD patterns recorded for all samples are presented in Fig. 5.

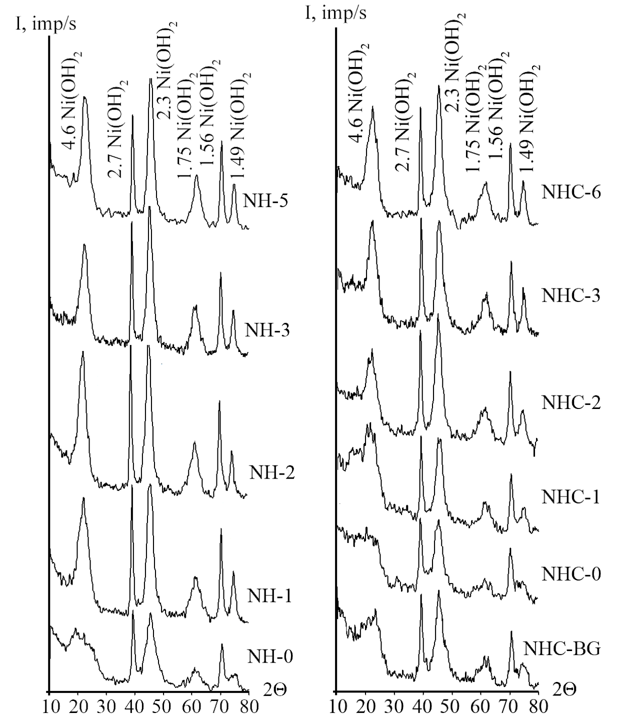

a *b*

Fig. 5. XRD pattern of nickel hydroxide samples: *a* – without the activator; *b* – with the activator

As can be seen, the effect of the aging process is rather significant. Samples that were not subjected to aging almost do not show the first peak for (001) (4.6 Å), Fig. 5, *a*. The same is observed for planes (102) (1.75 Å) and (111) (1.49 Å). This shows that ordering takes planes along the X and Z axes. It can be said that the number of defects decreases, as the intensity of all peaks increases with prolonged aging, and the background level decreases. The background here is the signal intensity between characteristic reflexes of the planes, which characterizes the number of defects and defective zones of crystals. It is interesting that the presence of activator does not affect the aging rate, as samples with the activator – Fig. 5, *b* show the same major changes during aging.

It should be noted that with prolonged aging time, the intensity of the peaks for (100) (2.7 Å) and (101) (2.3 Å) planes increase first, but then start to decrease. This is particularly characteristic for the peak (100) (2.7 Å).

For the most pronounced peaks (100) (2.7 Å) and (101) (2.3 Å), the block sizes were calculated, which are the average sizes of crystals with the correct crystal lattice in polycrystals of nickel hydroxides depending on aging time and are presented in Fig. 6.

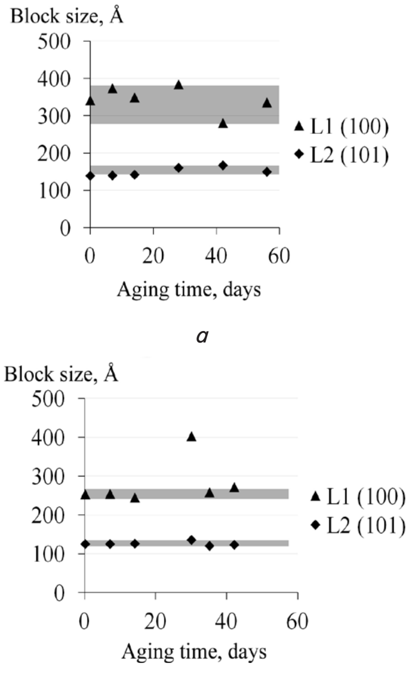

Fig. 6. Block sizes of (100) (2.7 Å) and (101) (2.3 Å) planes depending on aging time: *a* – without the activator; *b* – with the activator

Analysis of the results presented in Fig. 6 allows to draw a conclusion regarding aging rate and change in block size. The first conclusion – the block size is almost unaffected by the aging of nickel hydroxide powder. In case of all measurements, the corridors of size changes are shown, which are rather narrow Fig. 6 *a*, *b*. It should be noted that one value for the powder with the activator ((100) plane) was not taken into account, as it's a clear measurement error. Thus, the average values for nickel hydroxide powder are: 345 Å+/– 18 % (100) plane, 151 Å+/– 11 % (101) plane. For powder with the activator: 258 Å+/– 6 % (100) plane, 127 Å+/– 8 % (101) plane. As can be seen, the margin is rather small, which indicated that the main aging mechanism is ordering of defective zones and re-crystallization. From the presented graphs, it can also be seen that the second major mechanism is ordering along (001) plane (4.6 Å).

5. 1 Experimental results of electrochemical characterization of nickel hydroxide samples

Fig. 7 shows discharge curves for samples that were not subjected to aging and samples that were subjected to aging for the longest time. By analyzing the curves recorded for powders with and without the activator, it can be said that the average potential for discharge plateau is about 0.44–0.45 V for hydroxide without additives For fresh hydroxide with the activator, the average discharge potential is about 0.45 V, while for the sample that was aged for the longest time, the discharge potential is 0.36–0.38 V.

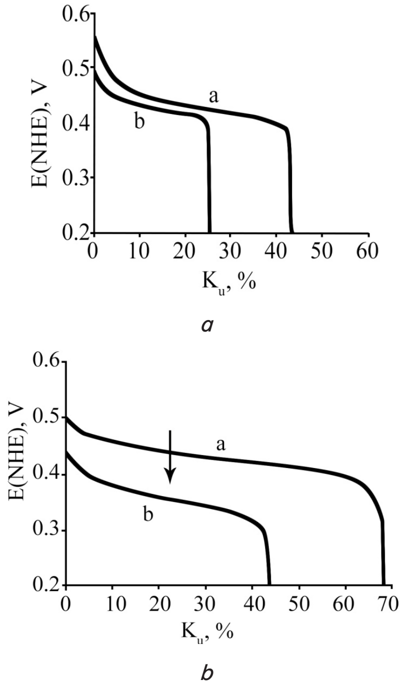

a

b

Fig. 7. Discharge curves for pure nickel hydroxide (a) and nickel hydroxide with the activator (*b*):
a — aging time — 0 days; *b* — aging time — 56 days

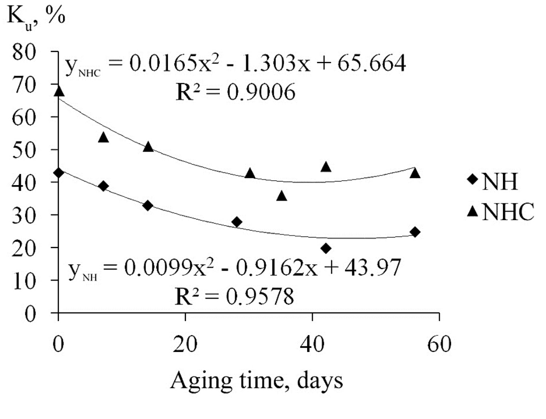

Fig. 8. Change of K_u with aging duration for pure nickel hydroxide (NH), for nickel hydroxide activated with cobalt (NHC) and approximated dependencies (solid lines) and approximation equations with determination coefficient R^2

Almost in all cases, the discharge time decreased with prolonged time of aging in alkali.

Fig. 8 shows the dependency of the active material utilization coefficient on aging time, for nickel hydroxide with and without the activator. Solid lines show approximated dependencies, where R^2 – determination coefficient. In both cases, the determination coefficient is higher than 90 % (more than 0.9), so, the presented equations provide a good description of dependency of K_u on aging time. As can be seen from approximated dependencies, Fig. 8, there is a sharp drop of the K_u value first, which then stabilizes somewhat. The dependency character is similar for both curves. The difference between the K_u values for powder without the activator in comparison to powder with the activator is almost unchanged and is about 20 % on average. The absolute decrease of K_u for pure powder is 18 %, relative – 42 % after 56 days. For powder with the activator, the absolute decrease of K_u is 25 %, and relative is 37 % after 56 days.

6. Discussion of results of structural and electrochemical activity studies of powders subjected to aging

According to the data obtained regarding structural changes during the aging process of active compounds, several principal facts can be outlined. First, the most pronounced change on XRD patterns is the increase of the first peak for (001) plane. An increase is also observed for all peaks, especial for (102) and (111) planes. Second, despite the obvious increase of peak intensities, for which block sizes were calculated ((100) and (101) planes), the size of ideal crystals along these planes is almost unchanged. This indicates that the major process during aging is ordering of the crystal structure with a decrease in the number of defects. This likely occurs because of re-crystallization of the defect zone on the boundary of ideal crystals in the polycrystal. The second major process, evidently, is ordering of the crystal lattice in (001) direction. Thus, it can be assumed that during aging, the removal of water and ions trapped between (001) planes. However, the latter should be proved separately.

Another important conclusion is that the presence of activator in the form of cobalt hydroxide does not have a significant effect on the aging process and its rate. This conclusion follows from the fact that structural changes of the powder are similar to those of pure $Ni(OH)_2$ powders.

During the study of the aging effect on discharge characteristics of the active material, it was revealed that aging leads to a significant decrease of specific characteristics. It was also revealed that the aging rate is almost independent of the presence of activator. Based on the dependency of the utilization coefficient on the aging time, it was revealed that the aging process is rapid initially, but its rate decreases over time. Additionally, the relative changes in K_u for powder with and without the cobalt hydroxide activator are close and are 42 and 37 %, respectively. The latter supports the previous conclusion on the presence of activator not having a major effect on the aging rate.

It is interesting that average discharge potentials for powders subjected to aging and those that were not, are close and are 0.44–0.45 V, which corresponds to the discharge of β-NiOOH: +0.450 V. At the same time, powders with the activator show significantly different discharge potential. For powder with the activator that was not subjected to aging, it is about 0.45 V [30]. On the contrary, the average discharge potential for samples with the activator is 0.38 V. This may indicate that during aging the re-crystallization can result in the formation of Ni-Co layered double hydroxide as a thin film on the surface of nickel hydroxide particles. While it might not be detected on the XRD pattern, owing to its small amount, it can have a significant impact on the discharge potential. This assumption is based on the fact that layered double hydroxides have a structure similar to α-$Ni(OH)_2$, which on charge transforms into γ-NiOOH (Fig. 1). γ-NiOOH has a lower discharge potential from +0.294 V to +0.384 V [31].

7. Conclusions

1. The aging process of nickel hydroxide in the alkali medium occurs through re-crystallization with decreasing number of structural defects, and ordering along (001) plane. The presence of activator in the form of cobalt hydroxide doesn't have a significant effect on the aging process and its rate, and structural changes.

2. The aging has a negative impact on specific electrochemical characteristics of $Ni(OH)_2$. The aging rate is high initially and decreases over time. For pure nickel hydroxide, the relative decrease of capacity K_u is 42 % after 56 days of aging in 4.5M KOH. For nickel hydroxide powder containing the activator in the form of cobalt hydroxide, the relative decrease of capacity is 37 % after 56 days of aging in 4.5M KOH.

References

1. Kovalenko V., Kotok V. Definition of effectiveness of β-$Ni(OH)_2$ application in the alkaline secondary cells and hybrid supercapacitors // Eastern-European Journal of Enterprise Technologies. 2017. Vol. 5, Issue 6 (89). P. 17–22. doi: 10.15587/1729-4061.2017.110390
2. Proton insertion reactions in layered transition metal oxides / Huggins R., Prinz H., Wohlfahrtmehrens M., Jorissen L., Witschel W. // Solid State Ionics. 1994. Vol. 70-71. P. 417–424. doi: 10.1016/0167-2738(94)90347-6
3. Kovalenko V., Kotok V., Bolotin O. Definition of factors influencing on $Ni(OH)_2$ electrochemical characteristics for supercapacitors // Eastern-European Journal of Enterprise Technologies. 2016. Vol. 5, Issue 6 (83). P. 17–22. doi: 10.15587/1729-4061.2016.79406
4. Nickel hydroxide obtained by high-temperature two-step synthesis as an effective material for supercapacitor applications / Kovalenko V. L., Kotok V. A., Sykchin A. A., Mudryi I. A., Ananchenko B. A., Burkov A. A. et. al. // Journal of Solid State Electrochemistry. 2016. Vol. 21, Issue 3. P. 683–691. doi: 10.1007/s10008-016-3405-2
5. Kotok V., Kovalenko V. The electrochemical cathodic template synthesis of nickel hydroxide thin films for electrochromic devices: role of temperature // Eastern-European Journal of Enterprise Technologies. 2017. Vol. 2, Issue 11 (86). P. 28–34. doi: 10.15587/1729-4061.2017.97371
6. Soft Electrochemical Etching of FTO-Coated Glass for Use in $Ni(OH)_2$ -Based Electrochromic Devices / Kotok V. A., Malyshev V. V., V. Solovov A., Kovalenko V. L. // ECS Journal of Solid State Science and Technology. 2017. Vol. 6, Issue 12. P. P772–P777. doi: 10.1149/2.0071712jss
7. Synthesis and characterisation of dyeintercalated nickelaluminium layereddouble hydroxide as a cosmetic pigment / Kovalenko V., Kotok V., Yeroshkina A., Zaychuk A. // Eastern-European Journal of Enterprise Technologies. 2017. Vol. 5, Issue 12 (89). P. 27–33. doi: 10.15587/1729-4061.2017.109814
8. The goldilocks electrolyte: examining the performance of iron/nickel oxide thin films as catalysts for electrochemical water splitting in various aqueous NaOH solutions / Browne M. P., Stafford S., O'Brien M., Nolan H., Berner N. C., Duesberg G. S. et. al. // Journal of Materials Chemistry A. 2016. Vol. 4, Issue 29. P. 11397–11407. doi: 10.1039/c6ta03903k
9. Glycerol oxidation on nickel based nanocatalysts in alkaline medium – Identification of the reaction products / Oliveira V. L., Morais C., Servat K., Napporn T. W., Tremiliosi-Filho G., Kokoh K. B. // Journal of Electroanalytical Chemistry. 2013. Vol. 703. P. 56–62. doi: 10.1016/j.jelechem.2013.05.021
10. Influence of temperature on the characteristics of Ni(II), Ti(IV) layered double hydroxides synthesised by different methods / Solovov V., Kovalenko V., Nikolenko N., Kotok V., Vlasova E. // Eastern-European Journal of Enterprise Technologies. 2017. Vol. 1, Issue 6 (85). P. 16–22. doi: 10.15587/1729-4061.2017.90873
11. New electrooxidation characteristic for Ni-based electrodes for wide application in methanol fuel cells / Barakat N. A. M., Yassin M. A., Al-Mubaddel F. S., Amen M. T. // Applied Catalysis A: General. 2018. Vol. 555. P. 148–154. doi: 10.1016/j.apcata.2018.02.016
12. Inkjet Printing NiO-Based p-Type Dye-Sensitized Solar Cells / Brisse R., Faddoul R., Bourgeteau T., Tondelier D., Leroy J., Campidelli S. et. al. // ACS Applied Materials & Interfaces. 2017. Vol. 9, Issue 3. P. 2369–2377. doi: 10.1021/acsami.6b12912
13. Calderón J. A., Jiménez J. P., Zuleta A. A. Improvement of the erosion-corrosion resistance of magnesium by electroless Ni-P/$Ni(OH)_2$-ceramic nanoparticle composite coatings // Surface and Coatings Technology. 2016. Vol. 304. P. 167–178. doi: 10.1016/j.surfcoat.2016.04.063
14. Effect of lightweight supports on specific discharge capacity of β-nickel hydroxide / Ramesh T. N., Jayashree R. S., Kamath P. V., Rodrigues S., Shukla A. K. // Journal of Power Sources. 2002. Vol. 104, Issue 2. P. 295–298. doi: 10.1016/s0378-7753(01)00919-3
15. Nickel hydroxides and related materials: a review of their structures, synthesis and properties / Hall D. S., Lockwood D. J., Bock C., MacDougall B. R. // Proceedings of the Royal Society A: Mathematical, Physical and Engineering Sciences. 2014. Vol. 2174. P. 20140792–20140792. doi: 10.1098/rspa.2014.0792

16. Srinivasan V., Cornilsen B. C., Weidner J. W. A nonstoichiometric structural model to characterize changes in the nickel hydroxide electrode during cycling // Journal of Solid State Electrochemistry. 2004. Vol. 9, Issue 2. P. 61–76. doi: 10.1007/s10008-004-0525-x
17. Fabrications of High-Capacity Alpha-$Ni(OH)_2$ / Young K.-H., Wang L., Yan S., Liao X., Meng T., Shen H., Mays W. // Batteries. 2017. Vol. 3, Issue 4. P. 6. doi: 10.3390/batteries3010006
18. Wehrens-Dijksma M., Notten P. H. L. Electrochemical Quartz Microbalance characterization of $Ni(OH)_2$-based thin film electrodes // Electrochimica Acta. 2006. Vol. 51, Issue 18. P. 3609–3621. doi: 10.1016/j.electacta.2005.10.022
19. Ramesh T. N., Kamath P. V. Synthesis of nickel hydroxide: Effect of precipitation conditions on phase selectivity and structural disorder // Journal of Power Sources. 2006. Vol. 156, Issue 2. P. 655–661. doi: 10.1016/j.jpowsour.2005.05.050
20. Cornilsen B. C., Karjala P. J., Loyselle P. L. Structural models for nickel electrode active mass // Journal of Power Sources. 1988. Vol. 22, Issue 3-4. P. 351–357. doi: 10.1016/0378-7753(88)80029-6
21. Cornilsen B. C., Shan X., Loyselle P. L. Structural comparison of nickel electrodes and precursor phases // Journal of Power Sources. 1990. Vol. 29, Issue 3-4. P. 453–466. doi: 10.1016/0378-7753(90)85018-8
22. Deciphering the Structural Transformations during Nickel Oxyhydroxide Electrode Operation / Casas-Cabanas M., Canales-Vázquez J., Rodríguez-Carvajal J., Palacín M. R. // Journal of the American Chemical Society. 2007. Vol. 129, Issue 18. P. 5840–5842. doi: 10.1021/ja068433a
23. Phase Stability of Nickel Hydroxides and Oxyhydroxides / Van der Ven A., Morgan D., Meng Y. S., Ceder G. // Journal of The Electrochemical Society. 2006. Vol. 153, Issue 2. P. A210. doi: 10.1149/1.2138572
24. Electrochemical Study of Zinc-Substituted Nickel Hydroxide / Tessier C., Faure C., Guerlou-Demourgues L., Denage C., Nabias G., Delmas C. // Journal of The Electrochemical Society. 2002. Vol. 149, Issue 9. P. A1136. doi: 10.1149/1.1495496
25. Jayashree R. S., Vishnu Kamath P. Supperession of the α→β nickel hydroxide transformation in concentrated alkali: Role of dissolved cations // Journal of Applied Electrochemistry. 2001. Vol. 31, Issue 12. P. 1315–1320. doi: 10.1023/a:1013876006707
26. Electrochemical Behavior of Cobalt Hydroxide Used as Additive in the Nickel Hydroxide Electrode / Pralong V., Delahaye-Vidal A., Beaudoin B., Leriche J.-B., Tarascon J.-M. // Journal of The Electrochemical Society. 2000. Vol. 147, Issue 4. P. 1306. doi: 10.1149/1.1393355
27. Yunchang D., Jiongliang Y., Zhaorong C. Cyclic voltammetry response of coprecipitated Ni(OH)2 electrode in 5 M KOH solution // Journal of Power Sources. 1997. Vol. 69, Issue 1-2. P. 47–54. doi: 10.1016/s0378-7753(97)02565-2
28. Nickel hydroxide ageing in different medias and its influence on electrochemical behavior in composition nickel electrode / Kotok V. A., Kozel N. D., Kovalenko V. L. et. al. // 8th Advanced batteries and accumulators – ABA-2007. Brno, 2007. P. 202–206.
29. Kovalenko V., Kotok V. Obtaining of Ni–Al layered double hydroxide by slit diaphragm electrolyzer // Eastern-European Journal of Enterprise Technologies. 2017. Vol. 2, Issue 6 (86). P. 11–17. doi: 10.15587/1729-4061.2017.95699
30. Barnard R., Randell C. F. Studies concerning charged nickel hydroxide electrodes: Part V. Voltammetric behaviour of electrodes containing β-Ni(OH)2 // Journal of Power Sources. 1983. Vol. 9, Issue 2. P. 185–204. doi: 10.1016/0378-7753(83)80032-9
31. Synthesis and behavior of Al-stabilized α-$Ni(OH)_2$ / Wang H., Tang Z., Liu Y., Lee C. // Transactions of Nonferrous Metals Society of China. 2009. Vol. 19, Issue 1. P. 170–175. doi: 10.1016/s1003-6326(08)60247-2